207

Advances in Powder Metallurgy & Particulate Materials - 1997

Proceedings of the 1997 International Conference on Powder Metallurgy & Particulate Materials sponsored by the Metal Powder Industries Federation and APMI International, June 29 - July 2, Chicago, Illinois.

Compiled by

Robert A. McKotch
President - Press Division
Gasbarre Products, Inc.

and

Richard Webb
Vice President - Operations
Norwalk Powdered Metals Company

METAL POWDER INDUSTRIES FEDERATION
APMI INTERNATIONAL
105 College Road East, Princeton, New Jersey 08540-6692
TEL (609) 452-7700 FAX (609) 987-8523

MODELING AND EXPERIMENTATION ON QUASI-ISOSTATIC PRESSING

Eugene A. Olevsky, Jerry C. LaSalvia and Marc A. Meyers
Institute for Mechanics and Materials
University of California, San Diego
9500 Gilman Dr., La Jolla CA 92093-0404

Abstract
A mathematical model of quasi-isostatic pressing (QIP - pressing in a granular pressure-transmitting medium) is developed. Stress-strain state and shape change inherent in QIP are analyzed. The regularities of change in the macroscopic aspect ratio and shape distortion are determined as functions of pressure transmitting medium and body porosities, as well as constitutive properties. QIP has an intermediate position between free upsetting, pressing in rigid die and isostatic pressing from the point of view of the stress-strain state and shape distortion. The experimental results on QIPing foam cylindrical bodies agree well with theoretical predictions.

1. Introduction

Uniaxial pressing with a pressure-transmitting medium (i.e. PTM) (Fig. 1) has been attracting attention [1]. Known as the Ceracon [2] or Quasi-Isostatic Pressing (i.e. QIP) process, it has been utilized industrially in manufacturing [3] and more recently, in combination with self-propagating high-temperature synthesis (i.e. SHS) [4-7]. When combined with SHS, QIP offers a relatively simple processing method by which hundreds of industrially-useful materials can be produced and shaped into engineering components. A granular pressure-transmitting medium (alumina or alumina with graphite powder) not only serves as a load transmitter, but also a natural thermal insulator which prevents substantial heat loss and minimizes temperature gradients during SHS.

In light of the current development of near-net-shape technologies, the analysis of both shape and volume changes under QIP is of considerable importance. The factors which influence the shape and volume change of a porous body include the initial porosities both the PTM and porous body, and their respective constitutive properties. The investigation of the effect of these factors on shape change during QIP is the objective of the present work.

2. Theoretical analysis of the shape change under quasi-isostatic pressing

Mechanical response of a nonlinear-viscous porous body can be described [8] by a rheological (constitutive) relationship connecting components of stress tensor σ_{ij} and strain rate tensor $\dot{e}_{ij}$:

$$\sigma_{ij} = A\left(\frac{\sqrt{\varphi\dot{\gamma}^2 + \psi\dot{e}^2}}{\sqrt{1-\theta}}\right)^{n-1}\left[\varphi\dot{e}_{ij} + \left(\psi - \frac{1}{3}\varphi\right)\dot{e}\delta_{ij}\right] \tag{1}$$

where A and n - are material creep parameters; φ and ψ are the shear and bulk normalized viscosity module, which depend on porosity θ (for example, following [10-12], $\varphi = (1-\theta)^2$, $\psi = \frac{2}{3}\frac{(1-\theta)^3}{\theta}$); δ_{ij} is a Kronecker symbol ($\delta_{ij} = 1$ if i=j and $\delta_{ij} = 0$ if $i \neq j$); $\dot{e}$ is the first invariant of the strain rate tensor, i.e. sum of tensor diagonal components: $\dot{e} = \dot{e}_{11} + \dot{e}_{22} + \dot{e}_{33}$.

For this analysis, the constitutive behavior of the PTM is assumed to be elastic, while that of the porous body is assumed to be nonlinearly-viscous. It is also assumed that the stresses are uniform within both the PTM and porous body. For simplicity, a cylindrical geometry is assumed, and cylindrical coordinate system is used throughout this paper (Fig.1).

In cylindrical coordinates, the volume-change rate $\dot{e}$ and the shape-change rate $\dot{\gamma}$ are given by:

$$\dot{e} = \dot{e}_{zz} + 2\dot{e}_{rr} = \left[1 + 2\left(\frac{\dot{e}_{rr}}{\dot{e}_{zz}}\right)\right]\dot{e}_{zz} = \frac{\dot{\theta}}{1-\theta} \tag{2}$$

$$\dot{\gamma} = \sqrt{\frac{2}{3}}\left|\dot{e}_{zz} - \dot{e}_{rr}\right| = \sqrt{\frac{2}{3}}\left|1 - \left(\frac{\dot{e}_{rr}}{\dot{e}_{zz}}\right)\right|\left|\dot{e}_{zz}\right| \tag{3}$$

where $\dot{e}_{zz}$, $\dot{e}_{rr}$, and θ are the axial strain rate, radial strain rate, and porosity, respectively. For a cylindrical specimen, the axial and radial strain-rates are given by:

$$\dot{e}_{zz} = \frac{\dot{H}}{H}; \dot{e}_{rr} = \frac{\dot{R}}{R} \tag{4}$$

where H and R are the instantaneous cylinder height and radius. Equation (3) gives the following relationship for the shape-change rate:

$$\dot{\gamma} = \sqrt{\frac{2}{3}}\left|\frac{\dot{H}}{H} - \frac{\dot{R}}{R}\right| \tag{5}$$

This expression will be used to derive relationships between the height and radius of the cylindrical specimen and porosity.

It is further assumed that the presence of the porous cylindrical body within the PTM provides a negligible effect on its state-of-stress as a result of the applied axial load. This is equivalent to imagining the porous cylindrical body embedded in an infinitely-extended PTM with a far-field applied stress σ_{zz}^{∞} at its boundary. The PTM itself is assumed to be under the condition of uniaxial load with lateral confinement (i.e. pressing in a rigid die). Therefore, the sample can be considered under conditions of biaxial loading (Fig. 1).

For the PTM, the axial and radial stresses are related to the axial strain ε_{zz} by Hook's law and are given by:

$$\sigma_{zz} = \left[\frac{1-\nu}{(1+\nu)(1-2\nu)}\right]E\varepsilon_{zz} \tag{6}$$

$$\sigma_{rr} = \left[\frac{\nu}{(1+\nu)(1-2\nu)}\right]E\varepsilon_{zz} \tag{7}$$

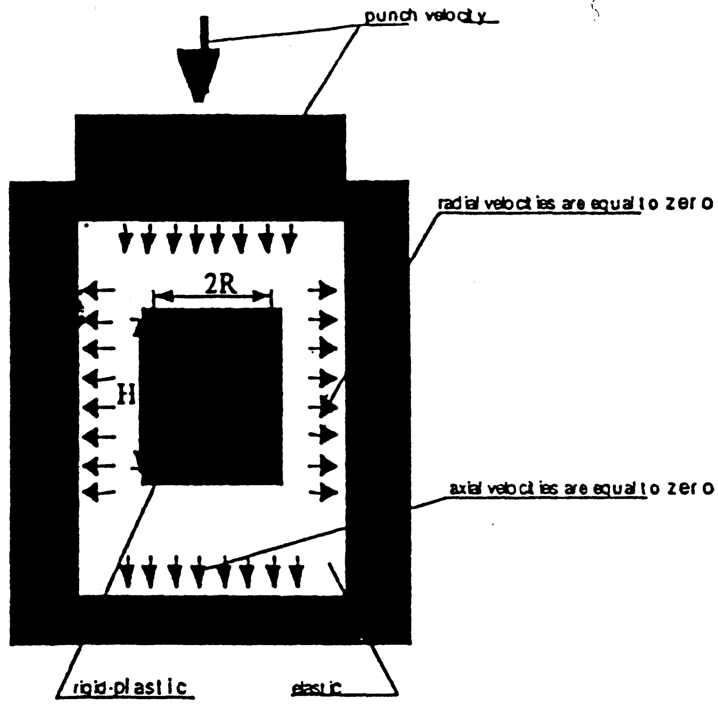

Fig. 1. Scheme of loading and the Boundary conditions for the finite-element formulation of the problem of QIP

where ν and E are the Poisson's ratio and Young's modulus for the PTM. These depend upon PTM porosity θ_p and are given by :

$$\nu = \frac{2-3\theta_p}{4-3\theta_p} \tag{8}$$

$$E = 4E_o\left[\frac{(1-\theta_p)^2}{4-3\theta_p}\right] \tag{9}$$

where E_o is the Young's modulus of the granular material making up the PTM. The ratio of the axial stress to the radial stress is therefore given by:

$$\frac{\sigma_{zz}}{\sigma_{rr}} = \frac{1-\nu}{\nu} = \frac{2}{2-3\theta_p} = k \tag{10}$$

The following expression for the axial/radial strain-rate ratio is valid:

$$\frac{\dot{e}_{rr}}{\dot{e}_{zz}} = \frac{k(2-3\theta)-2}{2(2-3\theta)-k(4-3\theta)} \tag{11}$$

If $k = \frac{2}{2-3\theta}$ (which means that $\theta = \theta_p$), then $\dot{e}_{rr} = 0$, and we have the conditions of pressing in a rigid die.

If k=1 (i.e., if $\theta_p = 0$ which means that PTM is an incompressible material), $\dot{e}_{rr} = \dot{e}_{zz}$, and we have the conditions of isostatic pressing.

If $k \to \infty$ (i.e., if $\theta_p = 2/3$) which approximately corresponds to the density of packed isomeric spherical particles then $\dot{e}_{rr} = \frac{3\theta-2}{4-3\theta}\dot{e}_{zz}$, and we have the conditions of free upsetting.

Combining Equations (2), (4), and (11) gives the following expression for the axial strain-rate in terms of the rate-of-change of porosity:

$$\dot{e}_{zz} = \frac{\dot{H}}{H} = \frac{1}{3}\left[\frac{2\theta_p + (1-3\theta_p)\theta}{(1-\theta_p)(1-\theta)}\right]\frac{\dot{\theta}}{\theta} \tag{12}$$

Combining Equations (2), (11), and (12) gives the following expression for the radial strain-rate in terms of the rate-of-change of porosity:

$$\dot{e}_{rr} = \frac{\dot{R}}{R} = \frac{1}{3}\left[\frac{\theta - \theta_p}{(1-\theta_p)(1-\theta)}\right]\frac{\dot{\theta}}{\theta} \tag{13}$$

The shape change rate can be represented as follows :

$$\dot{\gamma} = 2\sqrt{6}\left|\frac{(1-\theta)(1-k)}{2(2-3\theta)-k(4-3\theta)}\right||\dot{e}_{zz}| \tag{14}$$

Subtracting Equation (13) from (12), and integrating gives the following expression for the aspect ratio H/R:

$$\frac{\dot{H}}{H} - \frac{\dot{R}}{R} = \left(\frac{\theta_p}{1-\theta_p}\right)\frac{\dot{\theta}}{\theta} \Rightarrow \int_{\frac{H_o}{R_o}}^{\frac{H}{R}} d\ln\left(\frac{H}{R}\right) = \left(\frac{\theta_p}{1-\theta_p}\right)\int_{\theta_o}^{\theta} d\ln\theta$$

$$\Rightarrow \frac{H}{R} = \frac{H_o}{R_o}\left(\frac{\theta}{\theta_o}\right)^{\frac{\theta_p}{1-\theta_p}} \tag{15}$$

In deriving Equation (15), it was assumed that θ_p is constant. Equation (15) indicates that the change in the aspect ratio H/R does not depend upon the constitutive behavior of either the PTM or densified body, but depends only on the PTM porosity and the body's initial density and dimensional parameters.

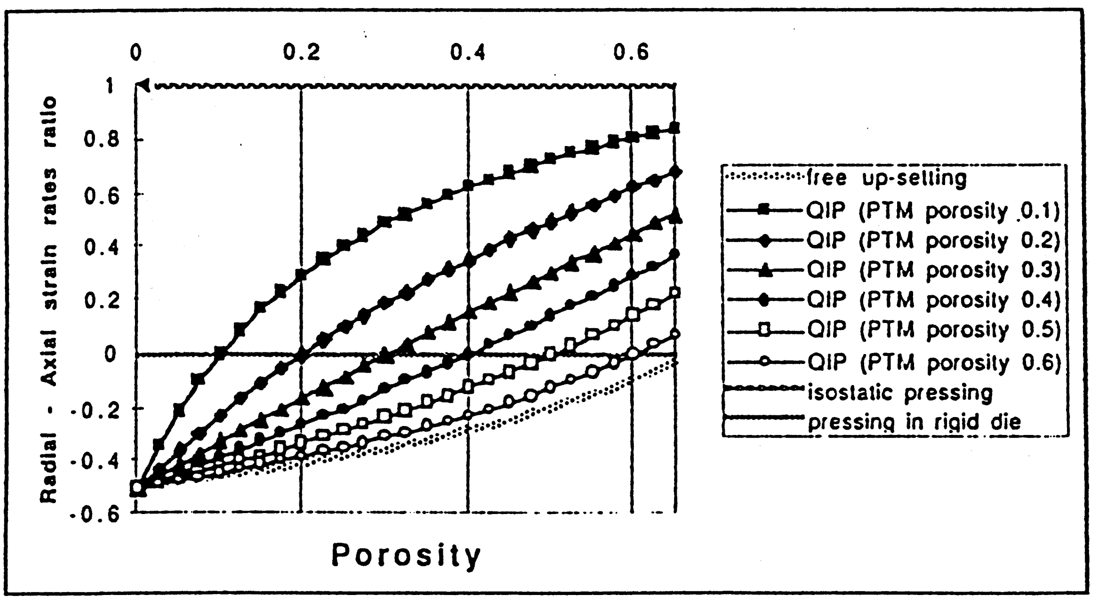

Fig.2. Shrinkage anisotropy as a function of specimen porosity under QIP

In Fig. 2, the curves are shown corresponding to the relationships between the radial-axial strain rate ratio and sample's porosity for various PTM porosities. For comparison, the curves corresponding to the conditions of free up-setting, pressing in a rigid die ($\frac{\dot{e}_{rr}}{\dot{e}_{zz}} = 0$) and isostatic pressing ($\frac{\dot{e}_{rr}}{\dot{e}_{zz}} = 1$) are shown too.

The data in Fig. 2 indicates that, for high PTM porosities, the porous material deformation mode under QIP can be closer to the conditions of free-upsetting rather than to the isostatic pressing ones.

Mostly, the radial-axial strain rate ratio, for $\theta_p > 0.5$, is in between the curves corresponding to pressing in a rigid die and free up-setting. This fact testifies the intensive shape change under QIP which is the distinctive feature of this process in comparison with the conventional containerless isostatic pressing.

3. Numerical analysis by the finite element method of shape distortion under qip

3.1. Numerical procedure

For the investigation of the shape distortion phenomenon under quasi-isostatic pressing, the boundary-value problem of pressing a cylindrical porous body in a rigid die filled by PTM (Fig. 1) is formulated. Material of PTM is assumed to be pure elastic, sample's material is rigid-plastic. The constitutive relationships for the sample's material correspond to Eq. 1 when $n = 0$.

The boundary conditions are represented by the flow velocities: at the upper punch axial velocities coincide with the punch's velocity; at the bottom of the die axial velocities are equal to zero. At the lateral walls of the die, radial velocities are equal to zero. Friction of PTM at the die and punch surfaces is neglected.

At the first stage, the problem based on assumption of linear-viscous properties of sample's material is solved. Then using some special iteration scheme [8] the solution is obtained in the framework of rigid-plastic rheology.

The initial porosity of PTM is assumed to be 0.65, the initial sample's porosity is 0.4.

3.2. Calculation results

The calculations show (Fig. 2a, 2b) that the ratio between constitutive parameters (Young modulus and yield limit) of PTM and sample influences the shape distortion (whereas the ratio between PTM and sample porosities effects the aspect ratio evolution). The influence of the ratio between PTM and sample porosities upon the shape distortion is less significant.

Under QIP of a sample with the high yield limit (for the porous body skeleton), e.g $E/\tau_0 < 50$, where E is a Young modulus of the PTM material and τ_0 is the sample's skeleton yield limit, the porous body keeps the shape close to cylindrical (Fig. 2a).

If the sample has a lower yield limit, e.g. $E/\tau_0 > 500$, its lateral surface takes a concave shape (Fig. 2b).

It should be noted that porous bodies undergo similar shape distortions under isostatic pressing in a container [9,10].

The indicated peculiarities of the shape change under QIP can be explained in the following way. For the lower sample yield limit, the resistance of the volume regions, where sample material is located, is lower than the resistance of the adjacent PTM. Therefore, PTM flows in the direction of smaller resistance, resulting the corresponding shape distortions. For the higher sample yield limit, the resistance of sample material is comparable to that of the adjacent PTM, therefore there are no dominant zones of the deformation flow and the sample keeps its cylindricity.

The investigation of the shape distortion factor requires usage of some model low-resistant material which can undergo considerable configuration changes under QIP. In such a way, the qualitative picture of this phenomenon can be better described. For this purpose, two kinds of foams were chosen as a model material. In the experiments, QIP of the Modulan and polyethylene foam was carried out.

The graphite powder transmitting medium was used in the experiments.

The polyethylene and Modulan foam samples were surrounded by graphite pressure transmitting medium and compacted.

The polyethylene foam cylindrical samples were subjected to a 5 kN load in the direction parallel (Fig. 3a)) and perpendicular (Fig. 3b)) to the sample axis.

The Modulan foam cylindrical sample was subjected to a 5 kN axial load (Fig. 3c)) and the Modulan foam prismatic sample was subjected to a 9.5 kN axial load during QIP (Fig. 3d)).

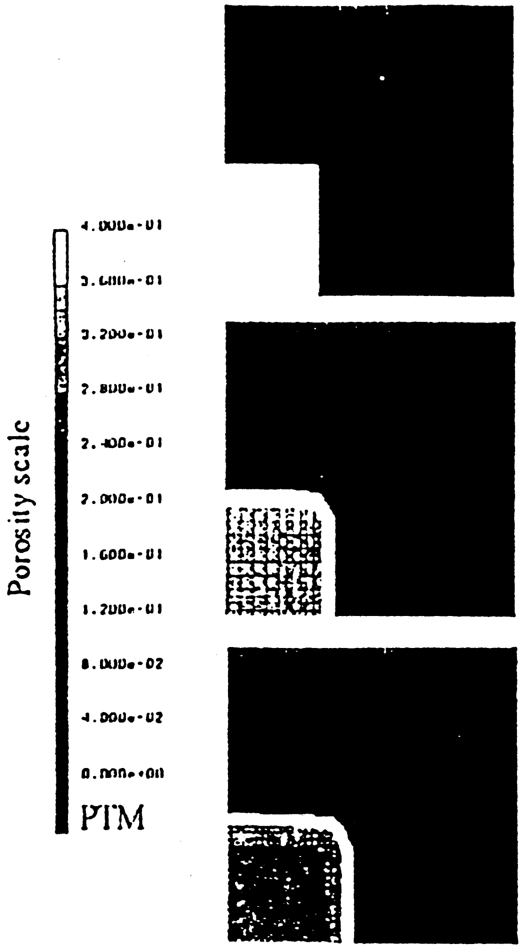

Fig. 2a. Calculation results for QIP of the porous sample with $E / \tau_0 < 50$;

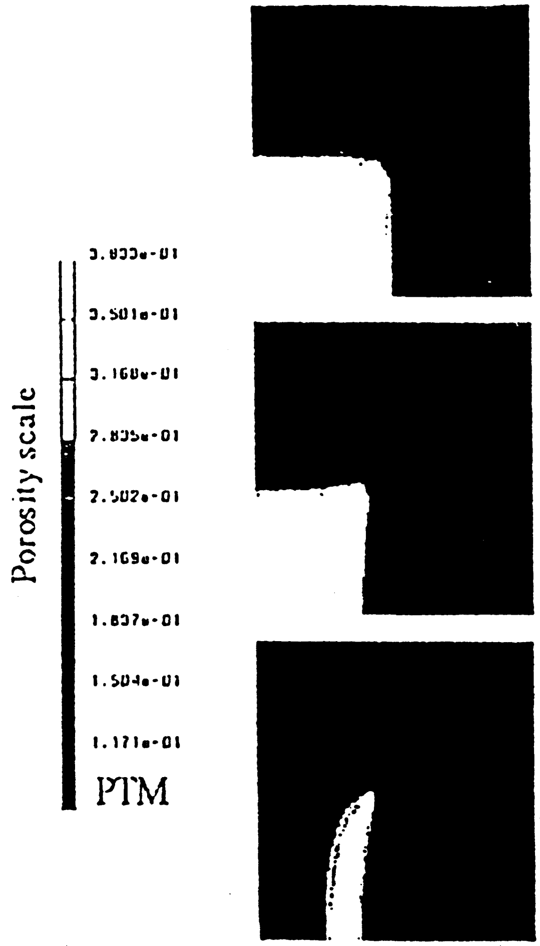

Fig. 2b. Calculation results for QIP of the porous sample with $E / \tau_0 > 500$;

4. Qualitative experimental analysis of the shape distortion under qip

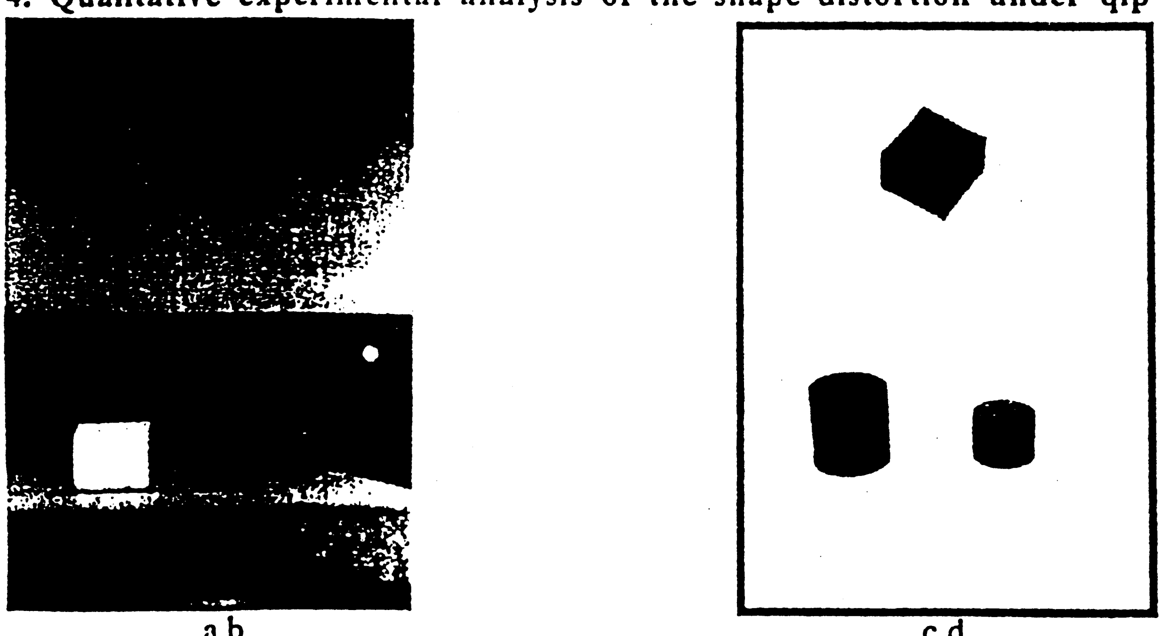

Fig. 3. Initial and final shape of the foam samples subjected to QIP
a. - polyethylene sample subjected to a 5 kN load in the direction parallel to the sample axis;
b. - polyethylene sample subjected to a 5 kN load in the direction perpendicular to the sample axis;
c. - Modulan foam cylindrical sample subjected to a 5 kN axial load during QIP;
d. - Modulan foam prismatic sample subjected to a 9.5 kN axial load during QIP.

The qualitative results of the experiments on QIPing foams confirm the results obtained by the finite element calculations.

The surface of the polyethylene foam, having a lower resistance, takes a concave shape after QIP (Fig. 3). A comparison of the results in Fig. 2a) and 2b) indicates that this effect does not depend on the macroscopic orientation of a sample. This confirms an idea formulated on the basis of the finite-element calculations: the main factor determining shape distortion under QIP is the relationship between constitutive properties of PTM particles and the porous sample skeleton.

The Modulan foam, having a higher resistance, keeps its cylindrical shape (Fig. 3d).

In the case of the prismatic shape, the slight concavity of the upper and lower end faces is compensated by the convexity of the lateral surface (Fig. 3c).

Conclusions

1. A mathematical model of the quasi-isostatic pressing (QIP) is developed.
2. The model predicts an essential shape change under QIP for large porosities of the pressure transmitting medium (PTM).
3. It is shown that, for most cases, the QIP deformation mode has an intermediate position between the deformation modes of pressing in rigid dies and free up-setting.
4. The results of the finite-element modeling of quasi-isostatic pressing are confirmed qualitatively by the model experiments on QIPing foam specimens.
5. The main factor determining shape distortion under QIP is the relationship between constitutive properties of PTM particles and the porous sample skeleton. The influence of the ratio between PTM and sample porosities upon the shape distortion is less significant.

Acknowledgment

The support of the NSF Institute for Mechanics & Materials, University of California, San Diego is gratefully acknowledged.

References

[1]. R.M. German, Powder Metallurgy Science, second ed., Metal Powder Industries Federation, Princeton NJ (1994)

[2]. R.V. Raman, S.V. Rele, S. Poland, J. LaSalvia, M.A. Meyers, and A.R. Niiler, The one-step synthesis of titanium-carbide tiles, *J. Metals*, N3, 23-25 (1995)

[3]. M. Ohyanagi, M. Fukushima, M. Koizumi, TiC-TiAl composite fabricated SHS - dynamic pseudo isostatic compaction through sand medium, *Hot Isostatic Pressing*, Andover MA, 289-294 (1996)

[4]. B. Mihelic, M. Dikic, R. Djekic, D. Uskokovic, Processing of compact materials by the use of self-propagating high-temperature synthesis and pseudo-hot isostatic pressing, *Materials Letters*, 13, 391-395 (1992)

[5]. J.C. LaSalvia and M.A. Meyers, Microstructure, properties, and mechanisms of TiC-Mo-Ni cermets produced by SHS, *Int. J. SHS*, 4, 43-57 (1995)

[6]. J.C. LaSalvia, D.K. Kim, R.A. Lipsett, and M.A. Meyers, Combustion synthesis in the Ti-C-Ni-Mo system: I. Macrokinetics and micromechanisms, *Met. Mat. Trans. A*, 26A, 3001-9 (1995)

[7]. J.C. LaSalvia and M.A. Meyers, Combustion Synthesis in the Ti-C-Ni-Mo system: II. Analysis, *Met. Mat. Trans. A*, 26A, 3011-19 (1995)

[8]. E. Olevsky, A. Maximenko, Nonstationary problems of the quasistatic theory of hardening plastic bodies, *Comp. Mat. Sci..*, 3, 247-253 (1994)

[9]. J. Besson, M. Abouaf, Rheology of porous alumina and simulation of hot isostatic pressing, *J. Amer. Ceram. Soc.*, 75[8], 2165-72, (1992)

[10]. A. Maximenko, E. Olevsky, Y. Panfilov, M. Shtern, Compaction of complex-shape powder details by isostatic pressing of porous billets with density nonuniformity, *Hot Isostatic Pressing*, L.Delaey, H.Tas (Eds.). Elsevier. 61-67 (1994)